INTERNATIONAL JOURNAL FOR NUMERICAL METHODS IN ENGINEERING
Int. J. Numer. Meth. Engng. **43**, 955–974 (1998)

VON NEUMANN STABILITY ANALYSIS OF BIOT'S GENERAL TWO-DIMENSIONAL THEORY OF CONSOLIDATION

MICHAEL I. MIGA *, KEITH D. PAULSEN AND FRANCIS E. KENNEDY
Thayer School of Enginerring, Dartmouth College, 8000 Cummings Hall, Hanover, NH 03755, U.S.A.

ABSTRACT

Von Neumann stability analysis is performed for a Galerkin finite element formulation of Biot's consolidation equations on two-dimensional bilinear elements. Two dimensionless groups—the Time Factor and Void Factor—are identified and these quantities, along with the time-integration weighting, are used to explore the stability implications for variations in physical property and discretization parameters. The results show that the presence and persistence of stable spurious oscillations in the pore pressure are influenced by the ratio of time-step size to the square of the space-step for fixed time-integration weightings and physical property selections. In general, increasing the time-step or decreasing the mesh spacing has a smoothing effect on the discrete solution, however, special cases exist that violate this generality which can be readily identified through the Von Neumann approach. The analysis also reveals that explicitly dominated schemes are not stable for saturated media and only become possible through a decoupling of the equilibrium and continuity equations. In the case of unsaturated media, a break down in the Von Neumann results has been shown to occur due to the influence of boundary conditions on stability. © 1998 John Wiley & Sons, Ltd.

KEY WORDS: Von Neumann; stability; consolidation; Galerkin finite element; soil consolidation; porous media; biphasic tissue mechanics

1. INTRODUCTION

In the field of soil mechanics, it is a well-known fact that soil subjected to an instantaneous load deforms in two distinct stages. The first stage is an instantaneous deformation at the contact area, followed by the second stage consisting of additional deformation caused by the settlement of soil over time.[1] The initial deformation is an elastic displacement of the solid matrix, with exiting pore fluid inducing the subsequent displacement. This process is known as soil consolidation and was first modeled in one dimension by Terzaghi.[2] Terzaghi considered the soil as a porous sponge-like material consisting of a solid matrix saturated with a pore fluid, usually water. Following Terzaghi, Biot presented a general theory for three-dimensional consolidation.[3]

Although consolidation theory has been primarily used in the field of soil mechanics, recently there has been an emerging interest in applying this theory to soft tissue mechanics.[4–7] Due to the viscoelastic nature of soft tissue, consolidation may prove to be an amenable modelling theory. By

* Corresponding to: Michael I. Miga, Thayer School of Engineering, Dartmouth College, 8000 Cummings Hall, Hanover, NH 03755, U.S.A. E-mail: michael-miga@dartmouth.edu

Contract/grant sponsor: National Institutes of Health; Contract/grant number: R01-NS33900

CCC 0029–5981/98/050955–20$17.50

Received 9 April 1997
Revised 12 January 1998

relating volumetric strain to media hydration, consolidation theory provides a potentially powerful tool for analysing the mechanical behaviour of tissue.

One of the most common computational schemes for consolidation problems is the Galerkin Finite Element Method (GFEM). While the formulation of the consolidation equations on finite elements is relatively straightforward and examples of computational successes abound in the literature,[4–6, 8, 9] only a modest amount of attention has been devoted to analysing the stability of this system of equations. In particular, Booker and Small[10] examined the stability of several time-stepping FEM formulations by using a Laplace transform approximation. In their analysis they assumed a fully saturated medium and concluded that schemes weighing implicit information more than explicit information are always stable. They also indicated that stable, explicitly dominated methods are possible and provided a time step criterion. Recently, Murad and Loula[11, 12] studied pore-pressure oscillations at certain spatial and temporal discretizations during the early stages of consolidation using equal order interpolation and Taylor–Hood[13, 14] mixed interpolation elements. With equal order interpolation they found that spurious spatial oscillations occur early in the consolidation process and are a result of an incorrect incompressibility constraint on the initial condition.[11] In addition, they indicate that although Taylor–Hood elements are stable they lead to an approximation for pore pressure which is one order lower in convergence than the displacement field. They also proposed a sequential Galerkin/Petrov–Galerkin post-processing technique to recover accuracy.[12] These mathematically elegant studies have been useful for highlighting certain computational features of FEM solutions of the consolidation equations especially for the Taylor–Hood type of interpolation scheme. However, the insights gained from a Von Neumann stability analysis have yet to be appreciated for FEM consolidation.

The goal of this paper is to explore Von Neumann stability analysis of the GFEM for the Biot problem using equal order interpolation elements (bilinear). While mixed elements have been demonstrated to offer certain attractive features *vis-à-vis* the suppression of transient pore pressure spatial oscillations, the practical utility of exploiting the simplest interpolation schemes (i.e. equal-order linear elements) is considerable especially in large-scale three-dimensional computations which occur in complex brain tissue models.[15, 16] As a result there is significant interest in and rationale for examining the numerical stability of equal-order linear elements and the Von Neumann approach is a previously untapped vehicle for exploring the discrete behaviour of the Biot equations in this regard. Although the underlying details would be different if other interpolation schemes were to be analysed in this way, the predominant discrete system behaviours which have been noted by others are demonstrated to be readily predicted with this analysis. New insights are also gained.

For example, the results concerning soil-dependent parameters show that materials with low shear moduli or low hydraulic conductivity decrease the stability of a Galerkin discrete form of the equations. Increasing the spatial resolution has a stabilizing effect while increasing temporal resolution does not stabilize in this case. In fact, the development of two dimensionless groups through the Von Neumann analysis highlights the finding that, all else being equal, it is the ratio of the time-step to the square of the space-step size which influences the presence and persistence of stable oscillations in the pore pressure. In a fully saturated media, the only reliable time-stepping method which always avoids all unstable and oscillatory temporal behaviour is found to be a fully implicit time-stepping scheme, whereas in unsaturated media, explicitly dominated methods are possible but only when the system of equations is decoupled. In addition, it is shown that reliable combinatory explicit/implicit schemes are possible provided the implicit information is more heavily weighted.

2. BASIC EQUATIONS

The theory of general consolidation proposed by Biot assumes that the soil is a linearly elastic isotropic solid experiencing small strains.[3] The theory also assumes that the pore fluid/liquid is incompressible, flows in accordance with Darcy's law and may contain gaseous voids (i.e. air bubbles) which makes the pore pressure medium potentially compressible. The equations incorporating two-dimensional plane strain mechanical equilibrium in Cartesian co-ordinates for a homogenous, linearly elastic continuum as described by Biot are:

$$G\nabla^2 u + \frac{G}{1-2v}\frac{\partial \varepsilon}{\partial x} - \alpha\frac{\partial p}{\partial x} = 0 \tag{1}$$

$$G\nabla^2 v + \frac{G}{1-2v}\frac{\partial \varepsilon}{\partial y} - \alpha\frac{\partial p}{\partial y} = 0 \tag{2}$$

where G is shear modulus, v is Poisson's ratio, α is the ratio of water volume extracted to the volume change of the soil, assuming the soil is being compressed and independent variables, u, v are the x, y displacements in the Cartesian plane, p is the pore fluid pressure and ε is the volumetric strain, $\varepsilon = \partial u/\partial x + \partial v/\partial y$.

In order to complete the continuum model, a constitutive relationship relating volumetric strain and fluid pressure is required. The final constitutive equation describing this relationship is

$$\nabla \cdot k\nabla p - \alpha\frac{\partial \varepsilon}{\partial t} - \frac{1}{S}\frac{\partial p}{\partial t} = 0 \tag{3}$$

which contains additional constants, k as the coefficient of hydraulic conductivity and $1/S$ as the amount of water which can be forced into the soil under pressure while the volume of soil is kept constant.

The first two terms in equation (3) provide the necessary coupling between volumetric strain and pore fluid pressure. The last term is created to account for the small gaseous voids in the media by making the pore pressure medium compressible.† Equations (1)–(3) can be written more compactly in terms of the unknown vector displacement $\mathbf{u}$ and pressure p

$$G\nabla \cdot \nabla\mathbf{u} + \frac{G}{1-2v}\nabla(\nabla \cdot \mathbf{u}) - \alpha\nabla p = 0 \tag{4a}$$

$$\alpha\frac{\partial}{\partial t}(\nabla \cdot \mathbf{u}) + \frac{1}{S}\frac{\partial p}{\partial t} - \nabla \cdot k\nabla p = 0 \tag{4b}$$

Standard weighted residual treatment of equation set (4) yields the coupled weak forms

$$\left\langle G\nabla\mathbf{u} \cdot \nabla\phi_i \right\rangle + \left\langle \frac{G}{1-2v}(\nabla \cdot \mathbf{u})\nabla\phi_i \right\rangle + \left\langle \alpha\nabla p\phi_i \right\rangle = \oint G\hat{n} \cdot \nabla\mathbf{u}\phi_i \, \mathrm{d}s + \oint \frac{G}{1-2v}\hat{n}(\nabla \cdot \mathbf{u})\phi_i \, \mathrm{d}s \tag{5a}$$

† Consistent with Biot's nomenclature, the term saturated will be used to describe incompressible media in the pore space (i.e. $\alpha = 1$, $1/S = 0$) while unsaturated will be used to refer to a compressible media in the pore space (i.e. $\alpha < 1$, $1/S > 0$)

$$\left\langle \alpha \frac{\partial}{\partial t}(\nabla \cdot \mathbf{u})\phi_i \right\rangle + \left\langle \frac{1}{S}\frac{\partial p}{\partial t}\phi_i \right\rangle + \left\langle k \nabla p \cdot \nabla \phi_i \right\rangle = \oint k\hat{n} \cdot \nabla p \phi_i \, \mathrm{d}s \tag{5b}$$

where $\langle \cdot \rangle$ indicates integration over the problem domain and $\oint$ is integration over its associated boundary. Here, ϕ_i is the ith member of a complete set of scalar functions of position, in particular, the usual C^0 local Lagrangian interpolant associated with finite elements. Discretization of (5) is completed in Galerkin fashion in space leading to ordinary differential equations which are integrated in time using the simple two-point weighting[17]

$$\int_{t_n}^{t_{n+1}} f(t)\,\mathrm{d}t = \Delta t\,[\theta f(t_{n+1}) + (1-\theta) f(t_n)]$$

where $\Delta t = t_{n+1} - t_n$ and $0 \leqslant \theta \leqslant 1$. In two-dimensional Cartesian co-ordinates this produces the two-level discrete system which is expressible as matrix equation

$$AU^{n+1} = BU^n + C^{n+\theta} \tag{6}$$

where A and B are composed of the submatrices

$$A_{ij} = \begin{bmatrix} \theta G\left\langle \frac{2(1-\nu)}{1-2\nu}\frac{\partial \phi_j}{\partial x}\frac{\partial \phi_i}{\partial x} + \frac{\partial \phi_j}{\partial y}\frac{\partial \phi_i}{\partial y} \right\rangle & \theta G\left\langle \frac{2\nu}{1-2\nu}\frac{\partial \phi_j}{\partial y}\frac{\partial \phi_i}{\partial x} + \frac{\partial \phi_j}{\partial x}\frac{\partial \phi_i}{\partial y} \right\rangle & \theta\alpha\left\langle \frac{\partial \phi_j}{\partial x}\phi_i \right\rangle \\ \theta G\left\langle \frac{2\nu}{1-2\nu}\frac{\partial \phi_j}{\partial x}\frac{\partial \phi_i}{\partial y} + \frac{\partial \phi_j}{\partial y}\frac{\partial \phi_i}{\partial x} \right\rangle & \theta G\left\langle \frac{2(1-\nu)}{1-2\nu}\frac{\partial \phi_j}{\partial y}\frac{\partial \phi_i}{\partial y} + \frac{\partial \phi_j}{\partial x}\frac{\partial \phi_i}{\partial x} \right\rangle & \theta\alpha\left\langle \frac{\partial \phi_j}{\partial y}\phi_i \right\rangle \\ \alpha\left\langle \frac{\partial \phi_j}{\partial x}\phi_i \right\rangle & \alpha\left\langle \frac{\partial \phi_j}{\partial y}\phi_i \right\rangle & \frac{1}{S}\left\langle \phi_j\phi_i \right\rangle + \\ & & \theta\Delta tk\left\langle \frac{\partial \phi_j}{\partial x}\frac{\partial \phi_i}{\partial x} + \frac{\partial \phi_j}{\partial y}\frac{\partial \phi_i}{\partial y} \right\rangle \end{bmatrix} \tag{7}$$

$$B_{ij} = \begin{bmatrix} \tilde{\theta} G\left\langle \frac{2(1-\nu)}{1-2\nu}\frac{\partial \phi_j}{\partial x}\frac{\partial \phi_i}{\partial x} + \frac{\partial \phi_j}{\partial y}\frac{\partial \phi_i}{\partial y} \right\rangle & \tilde{\theta} G\left\langle \frac{2\nu}{1-2\nu}\frac{\partial \phi_j}{\partial y}\frac{\partial \phi_i}{\partial x} + \frac{\partial \phi_j}{\partial x}\frac{\partial \phi_i}{\partial y} \right\rangle & \tilde{\theta}\alpha\left\langle \frac{\partial \phi_j}{\partial x}\phi_i \right\rangle \\ \tilde{\theta} G\left\langle \frac{2\nu}{1-2\nu}\frac{\partial \phi_j}{\partial x}\frac{\partial \phi_i}{\partial y} + \frac{\partial \phi_j}{\partial y}\frac{\partial \phi_i}{\partial x} \right\rangle & \tilde{\theta} G\left\langle \frac{2(1-\nu)}{1-2\nu}\frac{\partial \phi_j}{\partial y}\frac{\partial \phi_i}{\partial y} + \frac{\partial \phi_j}{\partial x}\frac{\partial \phi_i}{\partial x} \right\rangle & \tilde{\theta}\alpha\left\langle \frac{\partial \phi_j}{\partial y}\phi_i \right\rangle \\ \alpha\left\langle \frac{\partial \phi_j}{\partial x}\phi_i \right\rangle & \alpha\left\langle \frac{\partial \phi_j}{\partial y}\phi_i \right\rangle & \frac{1}{S}\left\langle \phi_j\phi_i \right\rangle + \\ & & \tilde{\theta}\Delta tk\left\langle \frac{\partial \phi_j}{\partial x}\frac{\partial \phi_i}{\partial x} + \frac{\partial \phi_j}{\partial y}\frac{\partial \phi_i}{\partial y} \right\rangle \end{bmatrix} \tag{8}$$

with $\tilde{\theta} = -(1-\theta)$ and U and C as the subvectors

$$U_j^n = \begin{Bmatrix} u_j(t_n) \\ v_j(t_n) \\ p_j(t_n) \end{Bmatrix} \tag{9}$$

$$C_i^{n+\theta} = \begin{Bmatrix} \hat{x} \cdot \oint \sigma_s(t_{n+\theta}) \cdot \hat{n}\phi_i \, ds \\ \hat{y} \cdot \oint \sigma_s(t_{n+\theta}) \cdot \hat{n}\phi_i \, ds \\ \Delta t \oint k \nabla p(t_{n+\theta}) \cdot \hat{n}\phi_i \, ds \end{Bmatrix} \tag{10}$$

In (10), $\sigma_s(t_{n+\theta})$ is the linearly elastic stress tensor evaluated at time $t_{n+\theta}$ (i.e. $\sigma_s(t_{n+\theta}) = \theta\sigma_s(t_{n+1}) + (1-\theta)\sigma_s(t_n)$) which expresses the boundary integrals in terms of normal stresses which are the natural boundary conditions for the mechanical equilibrium equations. Note that reaching this form requires some further manipulation of the boundary and volume terms emerging directly from the discrete versions of (5a).[16]

3. STABILITY ANALYSIS METHOD

Von Neumann stability analysis is an extremely useful method for understanding the propagation of errors in linear difference equations. By considering a general term in the closed-form Fourier series solution of the discrete system (prior to application of problem-dependent boundary and/or initial conditions), one can examine the potential for amplification of any of the possible Fourier modes which are sustainable on a discrete mesh. While problem dependent boundary/initial conditions may self-select a subset of these modes, the inevitable presence of rounding error precludes exclusion of any portions of the discrete Fourier spectrum in terms of stability analysis. Using this approach, the solution at space–time point (t_{n+1}, x_{i+1}, y_{j+1}) can be related to that at space–time point (t_n, x_i, y_j) through the relationship

$$u_{i+1,j+1}^{n+1} = e^{\lambda\Delta t} e^{j\sigma h} e^{j\beta h} u_i^n \tag{11}$$

where j in the exponential is $\sqrt{-1}$ and σh, βh are the dimensionless wave numbers in the x and y directions, respectively, on a uniform mesh with space–time discretization $x_{i+1} = x_i + h$, $y_{j+1} = y_j + h$, $t_{n+1} = t_n + \Delta t$. Stability analysis in this context then amounts to ensuring $|\gamma| \leqslant 1$, where $\gamma = e^{\lambda\Delta t}$, over all possible values of $\sigma h, \beta h$ ranging between 0 (infinite wavelength) and π (shortest wavelength on a discrete mesh).[17]

The difference relationships between nodal unknowns which result from the integration of the spatial variations appearing in submatrices A_{ij}, and B_{ij} in equations (7) and (8), when completely assembled for a single weighting function on a uniform mesh of bilinear elements, are given in column 2 of Table I.[18] These expressions are straight forward to produce and reminiscent of classical finite differences except for the additional averaging of neighbouring unknowns associated with finite element discretization. In Table I, the first column represents various Galerkin weighted residual terms with ϕ serving as the basis and weighting functions and i, j being the nodal indices. In the second column the i, j indexing in the difference expressions denotes a single-node location at (x_i, y_j) within the uniform mesh. Substituting equation (11) into these expressions produces the entries in column 3 which have been rewritten in terms of the identities presented in Table II.[18] Note that the quantities in Table II can be viewed as finite element discretization factors in the sense that they all approach unity as $\sigma h = \beta h \to 0$ (i.e. their continuum counterparts). Further, the finite-difference analogs can be obtained by dividing through by h^2 and setting the averaging factors A_x and A_y to unity.

Table I. Difference expressions and fourier descriptions

FEM term	Difference expression	Fourier description
$\sum u_j \left\langle \frac{\partial \phi_j}{\partial x} \frac{\partial \phi_i}{\partial x} \right\rangle$	$\frac{1}{6}(2u_{i,j+1} - u_{i+1,j+1} - u_{i-1,j+1}) + \frac{4}{6}(2u_{i,j} - u_{i+1,j} - u_{i-1,j}) + \frac{1}{6}(2u_{i,j-1} - u_{i+1,j-1} - u_{i-1,j-1})$	$A_y C_x^2 \sigma^2 h^2 u_{ij}$
$\sum u_j \left\langle \frac{\partial \phi_j}{\partial y} \frac{\partial \phi_i}{\partial y} \right\rangle$	$\frac{1}{6}(2u_{i+1,j} - u_{i+1,j+1} - u_{i+1,j-1}) + \frac{4}{6}(2u_{i,j} - u_{i,j+1} - u_{i,j-1}) + \frac{1}{6}(2u_{i-1,j} - u_{i-1,j+1} - u_{i-1,j-1})$	$A_x C_y^2 \beta^2 h^2 u_{ij}$
$\sum u_j \left\langle \frac{\partial \phi_j}{\partial y} \frac{\partial \phi_i}{\partial x} \right\rangle$	$\frac{1}{4}(u_{i-1,j+1} - u_{i+1,j+1}) + \frac{1}{4}(u_{i+1,j-1} - u_{i-1,j-1})$	$B_x B_y \sigma h \beta h u_{ij}$
$\sum u_j \left\langle \frac{\partial \phi_j}{\partial x} \phi_i \right\rangle$	$\frac{h}{12}(u_{i+1,j+1} - u_{i-1,j+1}) + \frac{h}{3}(u_{i+1,j} - u_{i-1,j}) + \frac{h}{12}(u_{i+1,j-1} - u_{i-1,j-1})$	$j A_y B_x \sigma h^2 u_{ij}$
$\sum u_j \left\langle \frac{\partial \phi_j}{\partial y} \phi_i \right\rangle$	$\frac{h}{12}(u_{i+1,j+1} - u_{i+1,j-1}) + \frac{h}{3}(u_{i,j+1} - u_{i,j-1}) + \frac{h}{12}(u_{i-1,j+1} - u_{i-1,j-1})$	$j A_x B_y \beta h^2 u_{ij}$
$\sum u_j \left\langle \phi_j \phi_i \right\rangle$	$\frac{h^2}{36}(u_{i+1,j+1} + 4u_{i,j+1} + u_{i-1,j+1}) + \frac{4h^2}{36}(u_{i+1,j} + 4u_{i,j} + u_{i-1,j}) + \frac{h^2}{36}(u_{i+1,j-1} + 4u_{i,j-1} + u_{i-1,j-1})$	$A_x A_y h^2 u_{ij}$

Table II. Definition of discretization factors for solutions of the form $u = u_{ij} e^{i(\sigma x + \beta y)}$ ($\Delta x = \Delta y = h$ is the mesh spacing)

$A_x = \frac{4 + 2\cos(\sigma h)}{6}$	$A_y = \frac{4 + 2\cos(\beta h)}{6}$
$B_x = \frac{\sin(\sigma h)}{\sigma h}$	$B_y = \frac{\sin(\beta h)}{\beta h}$
$C_x = \frac{\sin(\sigma h/2)}{\frac{\sigma h}{2}}$	$C_y = \frac{\sin(\beta h/2)}{\frac{\beta h}{2}}$

In the absence of any boundary conditions, matrix system (6) can now be recast as

$$\gamma \begin{bmatrix} \theta Ga & \theta Gb & \theta \alpha hc \\ \theta Gb & \theta Gd & \theta \alpha he \\ \alpha hc & \alpha he & \frac{1}{S} h^2 g + \theta \Delta t k f \end{bmatrix} \begin{Bmatrix} u_{ij} \\ v_{ij} \\ p_{ij} \end{Bmatrix}^n - \begin{bmatrix} \tilde{\theta} Ga & \tilde{\theta} Gb & \tilde{\theta} \alpha hc \\ \tilde{\theta} Gb & \tilde{\theta} Gd & \tilde{\theta} \alpha he \\ \alpha hc & \alpha he & \frac{1}{S} h^2 g + \tilde{\theta} \Delta t k f \end{bmatrix} \begin{Bmatrix} u_{ij} \\ v_{ij} \\ p_{ij} \end{Bmatrix}^n = \begin{Bmatrix} 0 \\ 0 \\ 0 \end{Bmatrix} \tag{12}$$

with

$$a = \frac{2(1-v)}{1-2v}A_y C_x^2 \sigma^2 h^2 + A_x C_y^2 \beta^2 h^2 \tag{13}$$

$$b = \frac{2v}{1-2v}B_x B_y \sigma h \beta h + B_x B_y \sigma h \beta h \tag{14}$$

$$c = \mathrm{j} A_y B_x \sigma h \tag{15}$$

$$d = \frac{2(1-v)}{1-2v}A_x C_y^2 \beta^2 h^2 + A_y C_x^2 \sigma^2 h^2 \tag{16}$$

$$e = \mathrm{j} A_x B_y \beta h \tag{17}$$

$$f = A_y C_x^2 \sigma^2 h^2 + A_x C_y^2 \beta^2 h^2 \tag{18}$$

and

$$g = A_x A_y \tag{19}$$

where A_x, A_y, B_x, B_y, C_x, and C_y are the discretization factors in Table II. Simplifying further the system becomes

$$\begin{bmatrix} (\theta(\gamma-1)+1)Ga & (\theta(\gamma-1)+1)Gb & (\theta(\gamma-1)+1)\alpha hc \\ (\theta(\gamma-1)+1)Gb & (\theta(\gamma-1)+1)Gd & (\theta(\gamma-1)+1)\alpha he \\ (\gamma-1)\alpha hc & (\gamma-1)\alpha he & (\gamma-1)\frac{1}{S}h^2 g + \\ & & (\theta\Delta t(\gamma-1)+\Delta t)kf \end{bmatrix} \begin{Bmatrix} u_{ij} \\ v_{ij} \\ p_{ij} \end{Bmatrix}^n = \begin{Bmatrix} 0 \\ 0 \\ 0 \end{Bmatrix} \tag{20}$$

For a non-trivial solution of (20), the determinant is required to vanish which yields

$$G^2(ad-b^2)\left(\theta\Delta tkf + \frac{1}{S}h^2 g + \frac{\Delta tkf}{\gamma-1}\right) + G\alpha^2 h^2(2bec - dc^2 - ae^2) = 0 \tag{21}$$

after dividing out the factor $(\theta(\gamma-1)+1)$ from the first two equations and the factor $(\gamma-1)$ in the third equation of (20). Solving (21) for γ leads to a more compact expression for the amplification factor shown here,

$$\gamma = 1 - \frac{\Delta tkf}{(\alpha^2 h^2/G)X + \theta\Delta tkf + (1/S)h^2 g} \tag{22}$$

where

$$X = \frac{2bec - dc^2 - ae^2}{ad - b^2} \tag{23}$$

After further manipulation, two dimensionless groups can be isolated,

$$\gamma = 1 - \frac{f}{(1/T_f)X + \theta f + (1/T_g)g} \tag{24}$$

where

$$T_f = \frac{Gk\Delta t}{\alpha^2 h^2} \tag{25}$$

$$T_g = \frac{\Delta t k}{h^2 (1/S)} \tag{26}$$

Interestingly, these two dimensionless numbers relate nicely to Biot's formulation of the consolidation constant C,[3]

$$\frac{1}{C} = \alpha^2 \frac{a^*}{k} + \frac{1/S}{k} \tag{27}$$

where $a^* = (1 - 2\nu)/(2G(1 - \nu))$ which in dimensionless form can then be approximated in terms of T_f and T_g as

$$\frac{h^2}{C \Delta t} \approx \frac{1}{T_f} + \frac{1}{T_g} \tag{28}$$

T_f is readily recognized as the soil mechanics dimensionless group known as the Time Factor, T,[1, 8, 9] for completely saturated soils (i.e. $\alpha = 1$, $(1/S) = 0$). In effect, this quantity represents the ratio of the rate of pore fluid transport to media compliance. The second dimensionless group is not as well established in the literature due to the tendency to consider only saturated soils. It relates the rate of pore fluid transport to void volume compliance and will be designated as the Void Factor, T_g, for the remainder of this paper. Note that a Void Factor value of infinity corresponds to a fully saturated medium (i.e. $\alpha = 1$, $1/S = 0$) while a very small Void Factor corresponds to a decoupled system ($\alpha < 1$, $1/S > 0$) where the pressure is propagated independently by the diffusion equation. By knowing only four dimensionless quantities, T_f, T_g, θ, and ν, stability can be assessed for all natural physical and discretization dependent parameters.

4. RESULTS

In this section we present the Von Neumann stability analysis for the 2-D consolidation equations in terms of the dimensionless Time Factor, T_f, Void Factor, T_g, Poisson's ratio, ν, and explicit/implicit weighting, θ. Each stability graph reported represents the amplification factor γ from equation (24) plotted as a function of the normalized spatial wave numbers which is referred to here as a stability plane. As a point of reference, $\sigma h^* = \beta h^* = 0{\cdot}2$ corresponds to a mesh sampling rate of 10 nodes/wavelength on the normalized axes shown in these figures.

In Figure 1, stability is quantified for varying Time Factor. The results indicate that increasing the Time Factor has a stabilizing influence on the solution which is characterized by the stability plane being pushed closer to zero for increasing T_f. With amplification factors less than unity, all Fourier spectral components decay with each successive time-step iteration causing the solution (and any associated rounding errors) to become smoother over time. However, as the Time Factor decreases, the decay of the high-frequency (large wave numbers) portions of the Fourier spectrum decreases serving to preserve the potential for spurious spatial oscillations over longer time scales. This behaviour can be readily illustrated using one of the predominant benchmark problems in the soil consolidation literature.[3]

Compression of a column of soil under a uniform load in its simplest form is a one-dimensional solution, however, it can be computed on two- and three-dimensional discretizations. Referring to

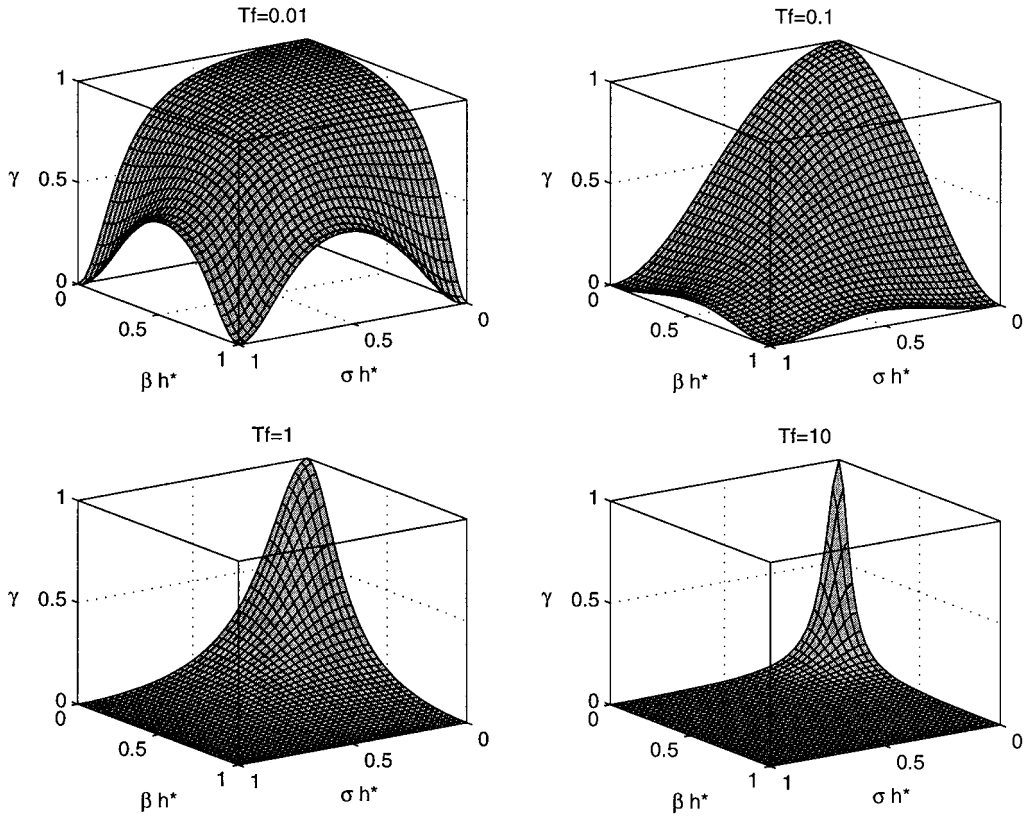

Figure 1. Stability plane for dimensionless Time Factor ($T_g = \infty$, $v = 0$, $\theta = 1$)

Figure 2, the boundary and initial conditions for this problem can be stated as:

Boundary 1: $u = 0$, $\sigma_{sy} = 0$, $\frac{\partial p}{\partial x} = 0$

Boundary 2: $\sigma_{sx} = 0$, $v = 0$, $\frac{\partial p}{\partial y} = 0$

Boundary 3: $\sigma_{sx} = 0$, $\sigma_{sy} = -p_0$, $p = 0$

Initial Conditions: at $t = 0$, $u = v = 0$ and $p = p_0$

To validate that the Galerkin finite element formulation given in equations (4)–(10) has been correctly implemented, comparisons between analytical and numerical solutions for this problem were performed and have been shown to be accurate within 2 per cent of applied load.[16] Figure 3 illustrates the effect of changing the Time Factor, T_f, on the computed pressure distribution at various points in time for the soil column example. It is clear from Figure 3 that decreasing T_f produces increased pore pressure oscillations while increasing this factor has the opposite effect consistent with the Von Neumann analysis presented in Figure 1. Further, these oscillations decay in time for both T_f values but damp faster as T_f increases, again as predicted. For a fixed set of physical properties and the same time-integration weighting, the critical parameter becomes the ratio of the time-step size to the square of the mesh spacing which governs the extent to which spatial oscillations in the pore pressure exist and persist. Increasing T_f under these conditions can be

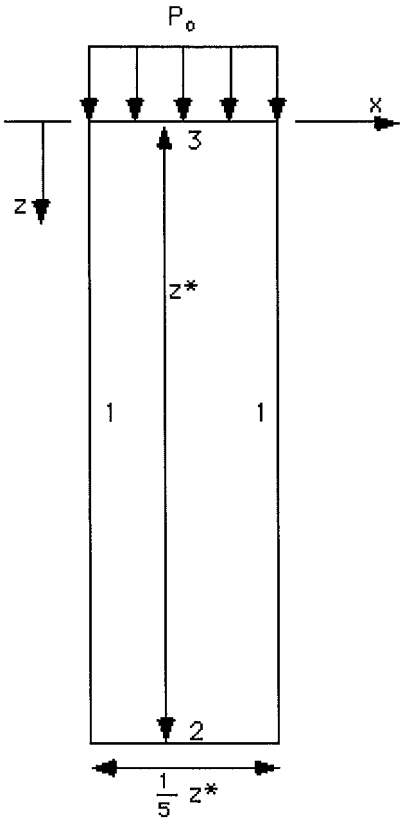

Figure 2. One-Dimensional analytical consolidation problem

equivalently accomplished by either increasing the time-step size or decreasing the mesh spacing; hence, the notion of transient, early-time pore pressure spatial oscillations must be considered in terms of the accompanying spatial resolution.

In Figure 4, it is shown that an increasing Void Factor also has an effect on stability which is analogous to the Time Factor for a fixed set of property parameters. The influence of the explicit/implicit weighting factor is demonstrated in Figure 5. The results indicate that explicitly dominated schemes are not possible for $T_g = \infty$. Also, in order to avoid temporal oscillations (i.e. $-1 < \gamma \leqslant 0$), a fully implicit weighting is required ($\theta = 1$); however, decreasing T_f or T_g can also be used to elevate the stability plane for a majority of wave numbers and is a viable avenue for reducing this effect for semi-implicit (meaning $\theta > 0{\cdot}5$) time-stepping schemes. An example of this special case is illustrated in Figures 6 and 7.

Figure 6 shows the stability plane calculated for two distinct values of T_f with an implicit/explicit weighting of $\theta = 0{\cdot}6$. In Figure 6, it is clear that the stability plane has risen by decreasing the Time Factor. The overall effect is to create a more stable environment for solution progression. This is quantified in Table III which presents a simple characterization of both stability planes in Figure 6 in terms of the average of the amplification factor over all wave numbers and the averages of the positive and negative amplification factors in each case. Using the soil column problem,

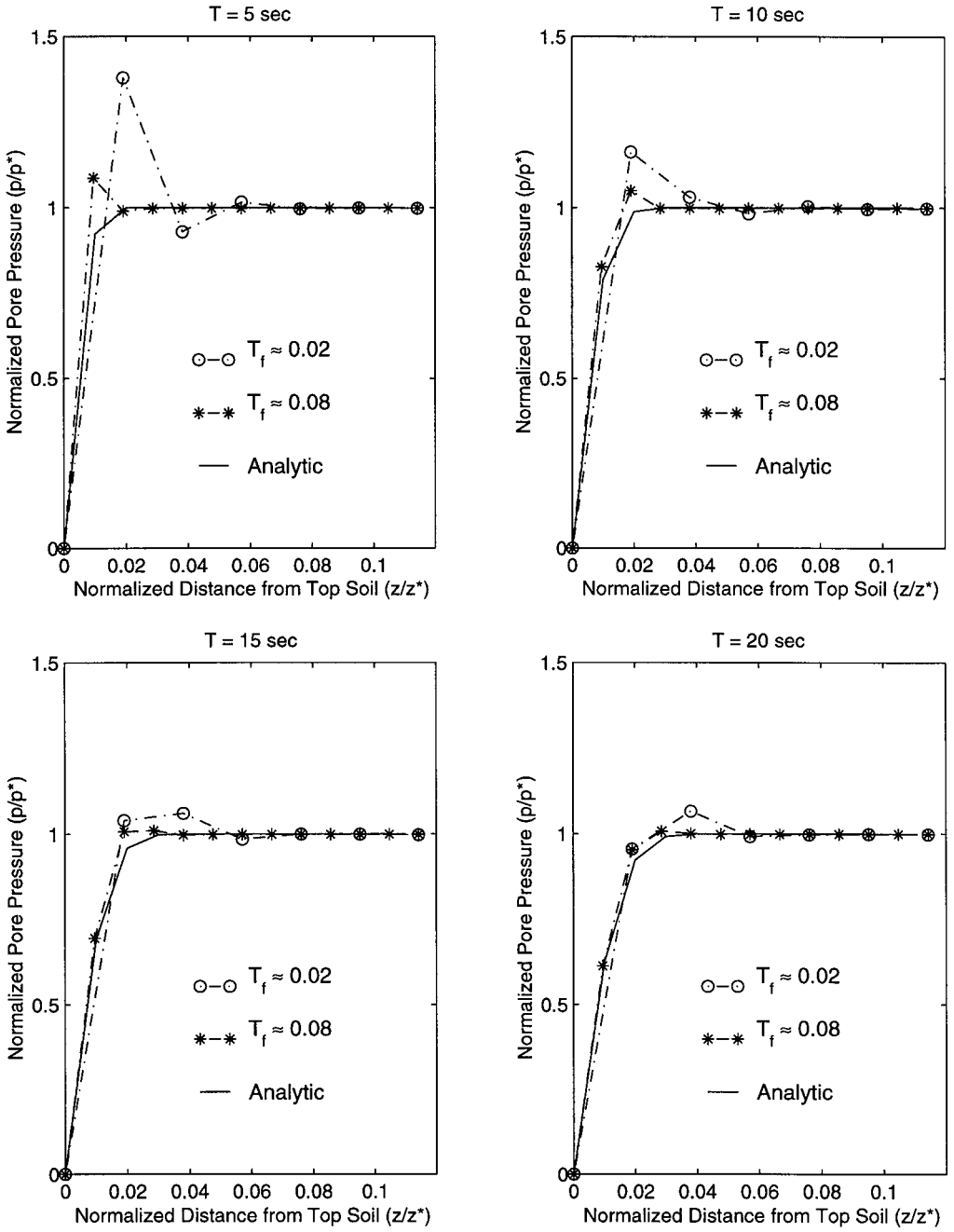

Figure 3. Pore pressure distribution with varying Time Factor ($T_g = \infty$, $v = 0$, $\theta = 1$)

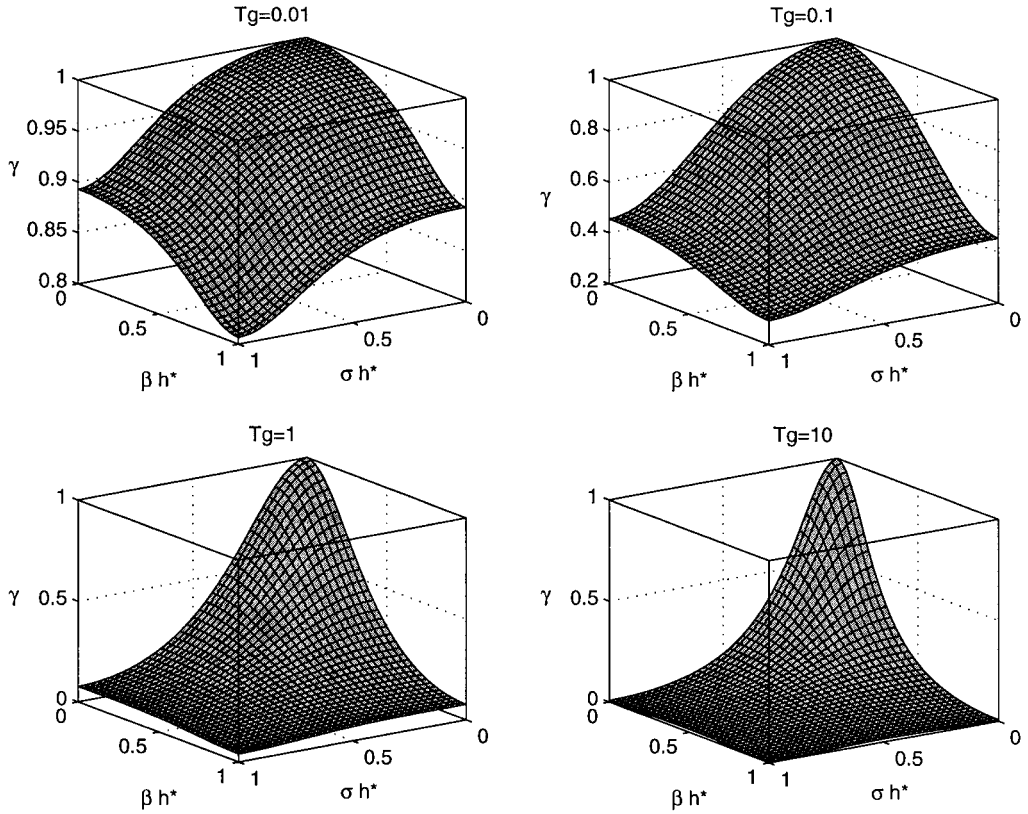

Figure 4. Stability plane for varying dimensionless Void Factor ($T_f = 1$, $v = 0$, $\theta = 1$)

Figure 7 demonstrates the effect of reducing the Time Factor on the pore pressure distribution in this case. In the first subfigure, T_f was changed by altering the time step size and computed solutions are compared to the analytic at the same point in time for fixed physical properties and spatial discretization. It is clear that by decreasing T_f a more accurate solution is calculated due to the improved suppresion of spurious high-frequency spectral components as predicted by Von Neumann. The second subfigure represents the value of pore pressure over time at a fixed point in space. Again as predicted by Von Neumann, temporal oscillations have been suppressed by decreasing T_f which reduces the number of Fourier modes with negative amplification factors. This example provides unique insight into the possibility of stable, accurate semi-implicit time-stepping schemes and is an excellent demonstration of the predictive power of the Von Neumann analysis.

It is also possible to relate T_f and T_g back to the physical property parameters assuming the spatial and temporal discretizations are fixed. For example, materials which readily deform in shear or have low hydraulic conductivity will have an adverse effect on stability. Materials exemplifying these traits decrease the dimensionless Time Factor which has been shown to be unfavorable. Table IV provides a qualitative summary of the influence of the primary physical and discretization parameters on stability.

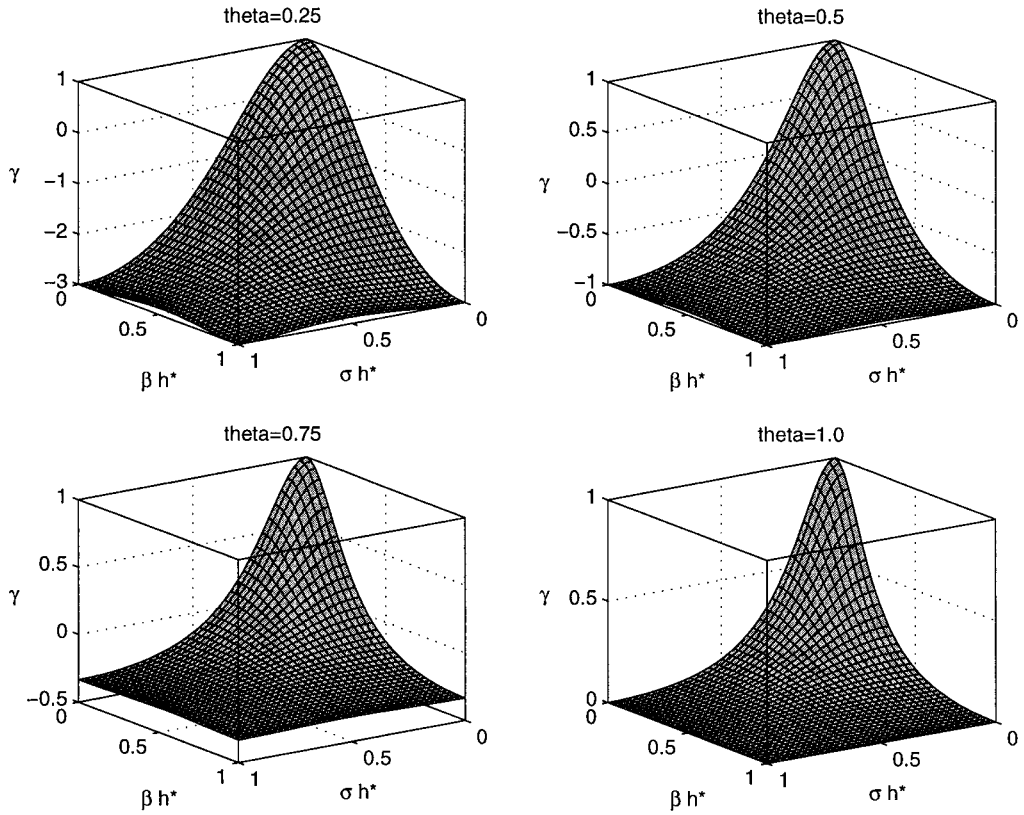

Figure 5. Stability plane for varying explicit/implicit weighting ($T_f = 1$, $T_g = \infty$, $v = 0$)

Another interesting finding is that stable time stepping can only result from an implicitly dominated scheme (i.e. $\theta > 0{\cdot}5$ or semi-implicit) for a saturated medium. In addition, to avoid temporal oscillations in general, the scheme must be fully implicit (i.e. $\theta = 1$). Reliable semi-implicit schemes are only possible for the case highlighted by Figures 6 and 7 which has analogous examples using the Void Factor (i.e. $1/S > 0$, $\alpha < 1$). Similar to T_f, decreasing T_g can have the effect of raising the stability plane which could satisfy $0 < \gamma < 1$ for the excited Fourier modes. However, increasing the $1/S$ term (i.e. decreasing the Void Factor) can result in a breakdown in the Von Neumann analysis due to boundary condition effects which are not considered.

Figure 8 is an example of a set of parameters where Von Neumann predicts a stable solution when in fact the method is unstable in practice. Recall that in the case of a small Void Factor, pressure is being driven by diffusion and the system is approaching a decoupled set of equations (i.e. $\alpha = 0$). Some insight can be gained as to how the boundary conditions serve to destroy stability for explicitly dominated methods in the coupled unsaturated system by examining the decoupled equations. The decoupled system can be written as

$$\nabla \cdot \sigma_s = 0 \tag{29}$$

$$\frac{1}{S}\frac{\partial p}{\partial t} - \nabla \cdot k \nabla p = 0 \tag{30}$$

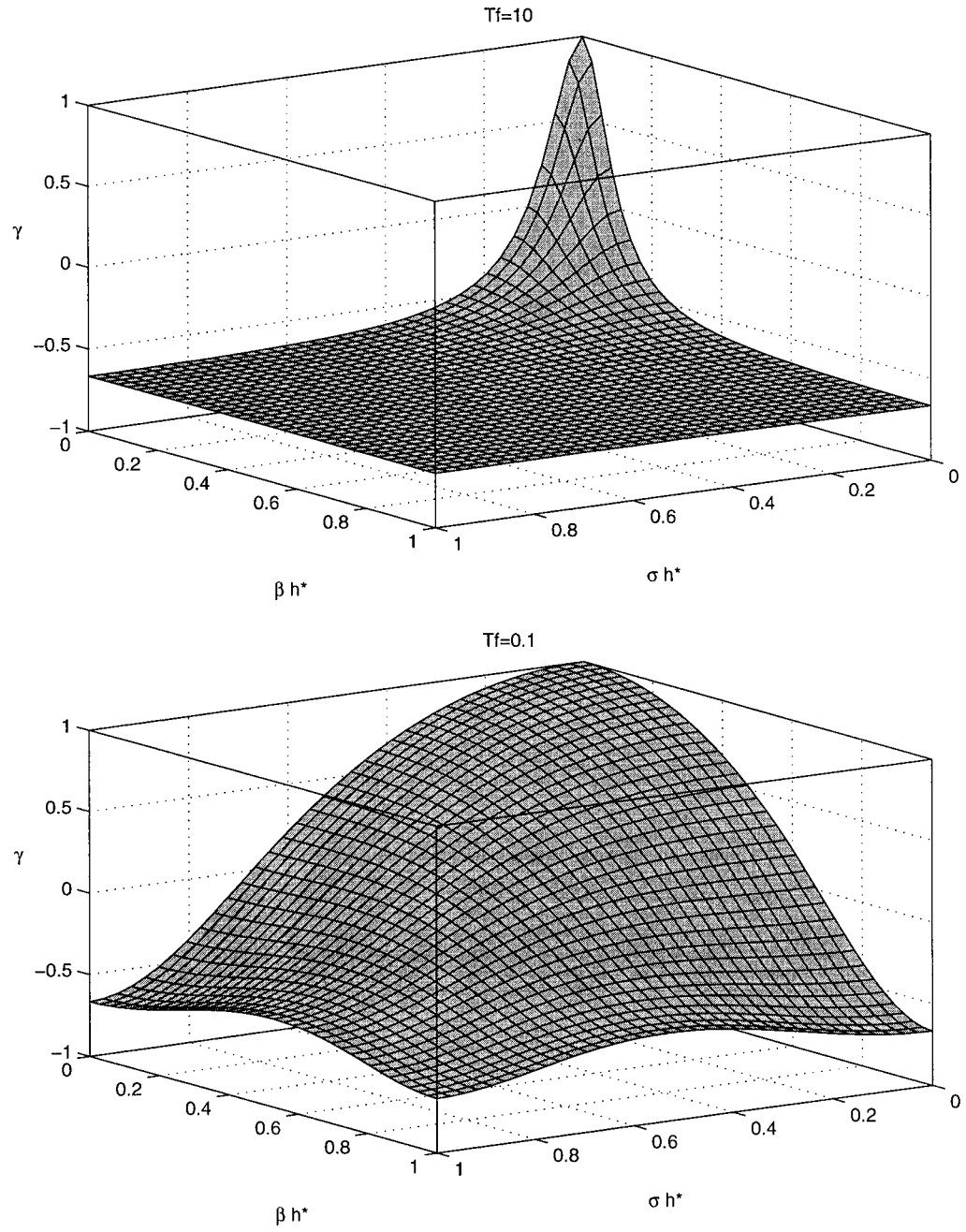

Figure 6. Stability plane for varying T_f weighting in the case of a semi-implicit time integration ($T_g = \infty$, $v = 0$, $\theta = 0{\cdot}6$)

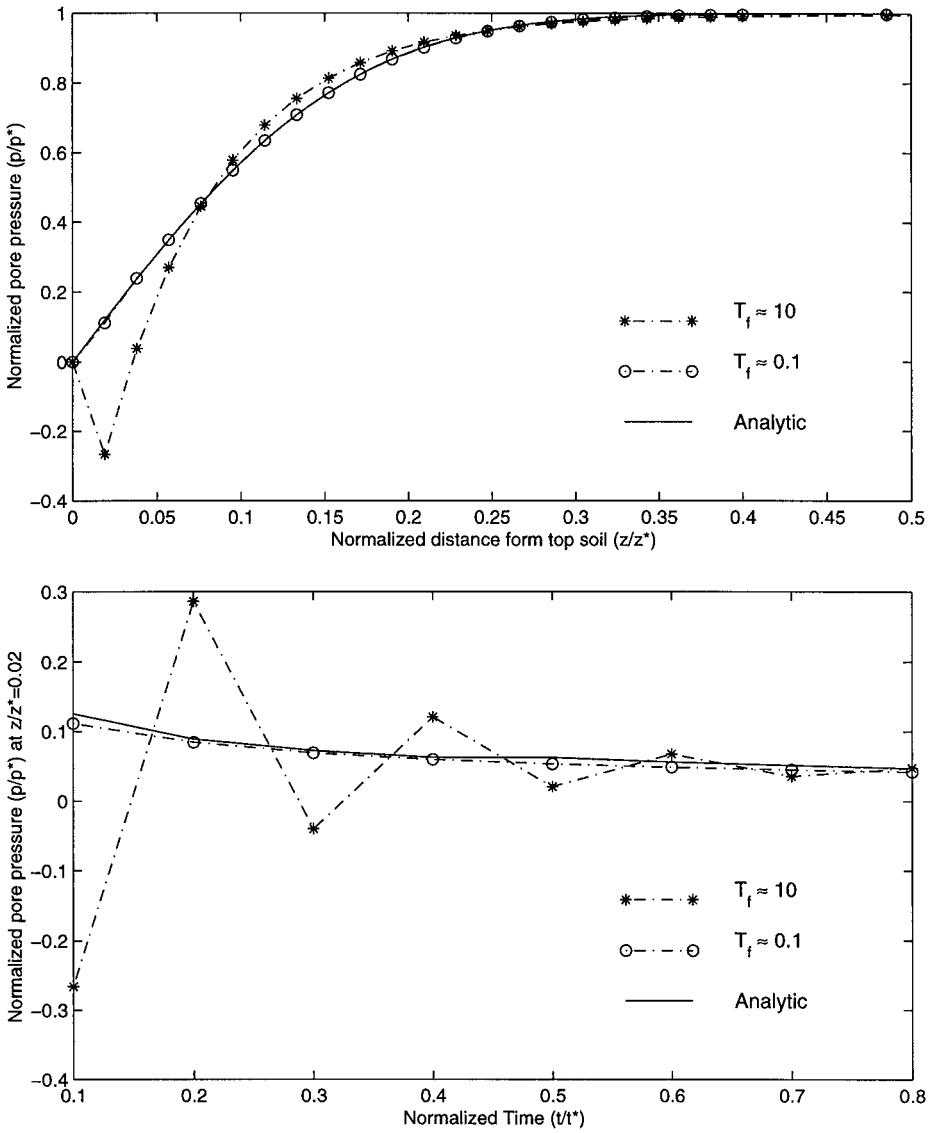

Figure 7. Pore pressure distribution with varying Time Factor in the case of a semi-implicit time integration ($T_g = \infty$, $v = 0$, $\theta = 0{\cdot}6$)

where σ_s is the stress tensor. Following the same space–time discretization approach as described previously, the equilibrium equations can be written as

$$\theta A U^{n+1} = \tilde{\theta} A U^n + C^{n+\theta} \tag{31}$$

The next task in solving such a system would be to implement boundary conditions, changing (32) to

$$\theta A' U^{n+1} = \tilde{\theta} A^* U^n + C^{n+\theta} \tag{32}$$

Table III. Quantification of stability plane elevation in semi-implicit time integration

Amplification factor	Average value (no. of values) $T_f = 10$	Average value (no. of values) $T_f = 0{\cdot}1$
Whole plane	−0·62 (1369)	−0·01 (1369)
Positive plane	0·41 (17)	0·48 (595)
Negative plane	−0·63 (1352)	−0·38 (774)

Table IV. Summary of stability effects from varying physical and independent parameters

Parameter	Parameter description	Stability effect of increasing
G	Shear modulus	Favorable
v	Poisson's ratio	Negligible
k	Hydraulic conductivity	Favorable
$\frac{\alpha}{1/S}$	Media saturation	Favorable
h	Average element length	Unfavorable
Δt	Time step size	Favorable
θ	Weighting of explicit/implicit Info.	Favorable

The only difference between A' and A^* would be the rows corresponding to Dirichlet boundary conditions. After the incorporation of boundary data (which must contain at least one Dirichlet condition in order to maintain solution uniqueness) the iteration matrix, P,

$$P = \frac{\tilde{\theta}}{\theta} A'^{-1} A^* \tag{33}$$

which advances the solution in time has a maximum eigenvalue

$$\lambda_{\max} = \max\left[\mathrm{eig}(P)\right] = \max\left[\frac{\tilde{\theta}}{\theta}\mathrm{eig}(A'^{-1}A^*)\right] = \frac{\tilde{\theta}}{\theta}(1) = 1 - \frac{1}{\theta} \tag{34}$$

which is greater than one for $\theta < 0{\cdot}5$, hence, making the time evolution of the solution unstable for these conditions. From this analysis, the following extrapolation can be made:

$$\lim_{T_g \to 0, \alpha \to 0} \max\left[\mathrm{eig}(P)\right] \Rightarrow 1 - \frac{1}{\theta} \tag{35}$$

This is an important result and indicates that stable explicitly dominated schemes are only possible when the system of equations is decoupled (i.e. $\alpha = 0$). By doing so, the only stability limit considerations would arise from a classic diffusion equation analysis, in which case the stability plane shown in Figure 8 is representative of the amplification factor profile that would result. It should be noted that while setting $\alpha = 0$ does not represent soil consolidation in a physical sense as Biot originally intended, considering this condition does provide a more complete picture of the numerical stability of the full range of possibilities embodied within this mathematical framework.

The findings regarding an explicitly dominated time-stepping scheme for a saturated medium (i.e. $\alpha = 1$, $1/S = 0$) appear to conflict with those reported by Booker and Small. In Booker's

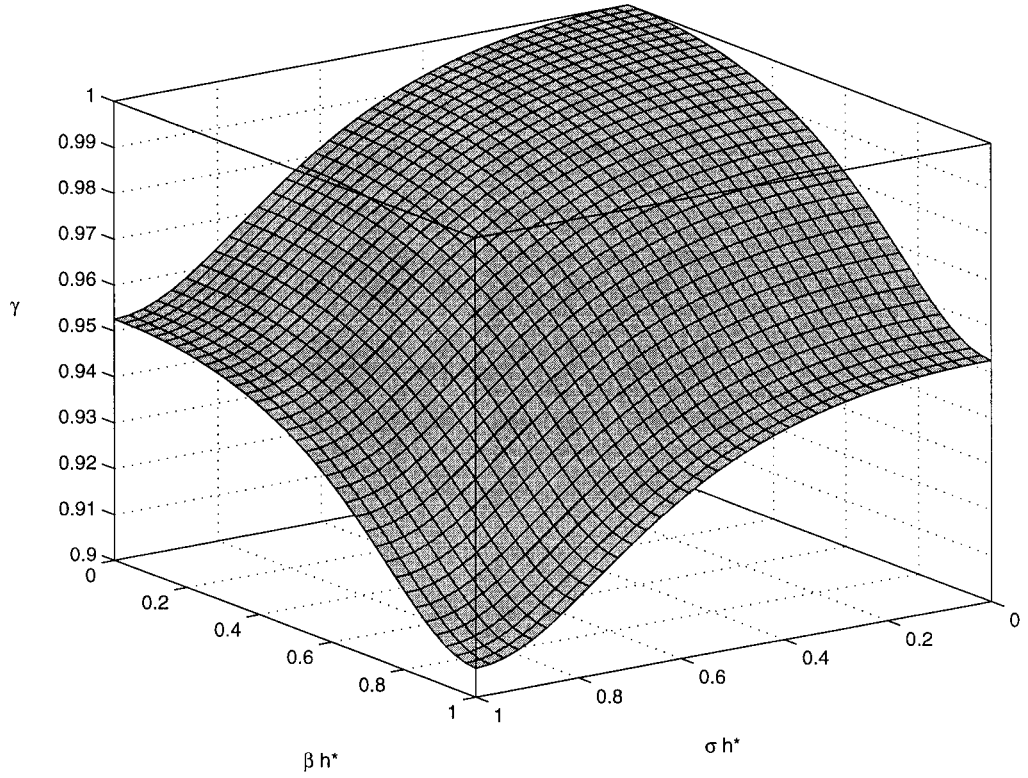

Figure 8. Example stability plane of Von Neumann analysis breakdown ($T_f = 5$, $T_g = 4e - 3$, $v = 0{\cdot}3$, $\theta = 0{\cdot}25$)

approximation, the possibility of an explicitly dominated method for a saturated media was suggested based on numerical calculations[10] which led to the conclusions that:

(i) $\theta \geqslant 0{\cdot}5$ always stable, and

(ii) $\theta < 0{\cdot}5$ is stable provided $\Delta t \leqslant \frac{0{\cdot}614 \times 10^{-4}}{(0{\cdot}5-\theta)}$

Figure 9 presents the stability plane resulting from the Von Neumann analysis using the same parameter space and physical constant values as Booker. Interestingly, over 99 per cent of wave numbers are within the stable range; however, there are certain wave numbers which will produce an instability. The discrepancy between Figure 9 and the results from Booker could occur if the Booker solution did not propagate long enough in time or if the initial conditions utilized did not excite the unstable Fourier modes shown to exist in Figure 9. Another possible explanation for the conflicting results could be a result of excessive solution restriction due to boundary conditions. Von Neumann analysis does not include boundary condition effects, and the mesh used by Booker has two nodes of every triangular element on a boundary, thus allowing only one degree of freedom per element. Any combination of all these reasons could explain the difference between the Von Neumann analysis presented here and the numerical experience recorded by Booker and Small.[10]

Murad and Loula also examined the stability characteristics of a Galerkin formulation of the consolidation equations for saturated media. They observed 'spurious oscillations in the pressure field in the early stage of consolidation for some combination of displacement and pore-pressure

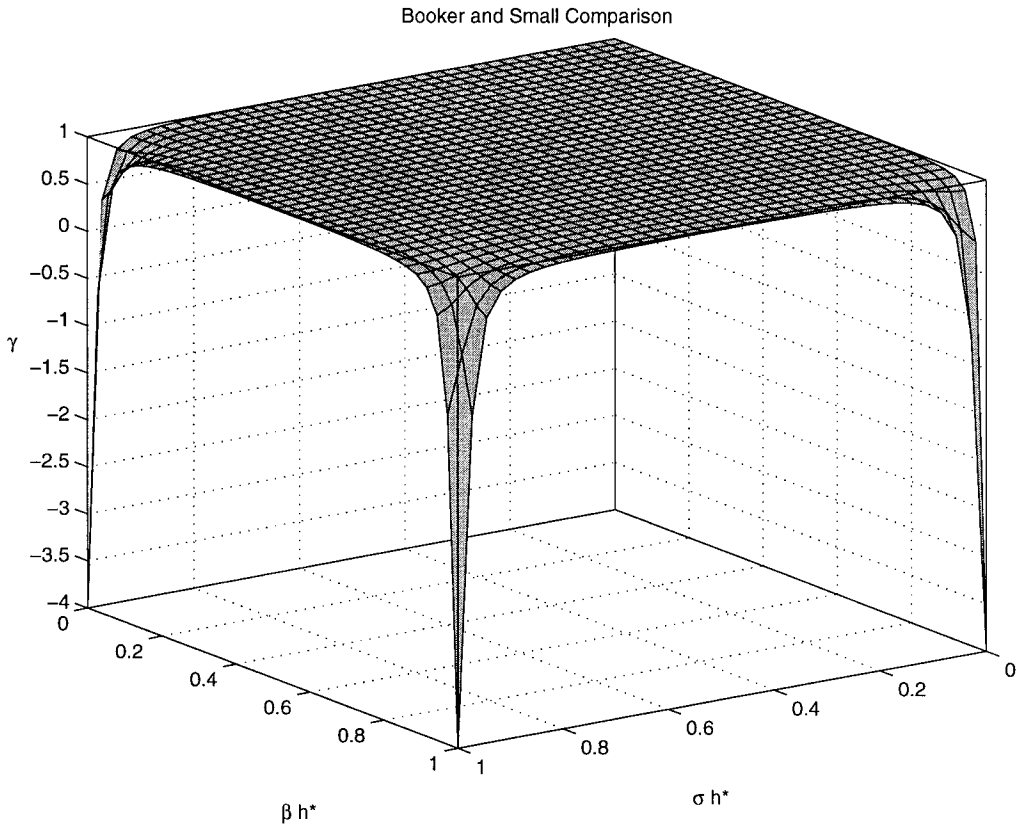

Figure 9. Stability plane for comparing Booker and Small results ($T_f = 3{\cdot}2e-4$, $T_g = \infty$, $v = 0{\cdot}25$, $\theta = 0{\cdot}2$)

finite element spaces'.[12] In their first paper, they use 'numerical analysis, based on the concept of elliptic projection of the exact solution as a comparison function, to derive error estimates of the Galerkin approximation'.[11] They go on to propose and implement a post-processing technique to rectify these oscillations.[12] Von Neumann analysis is also a useful tool in determining whether such post-processing is required. Using the parameter space values given by Murad and Loula which were found to precipitate spatial oscillations,[11] Figure 10 presents the stability plane as determined by Von Neumann. The predominant feature is that the amplification factor has a value of unity for virtually all wavenumbers. This would indicate strong neutrally stable characteristics for this spatial/temporal discretization. In this case, round-off error is not sufficiently suppressed and spurious spatial oscillations can develop from the jump conditions induced at the initial time step. By analysing spatial/temporal discretizations using the simple relationship given in (24), these spurious oscillations can be predicted.

5. CONCLUSIONS

This analysis reveals that the dominant dimensionless parameters affecting stability of the Galerkin FEM formulation of Biot's two-dimensional consolidation equations are the Time Factor, T_f, Void

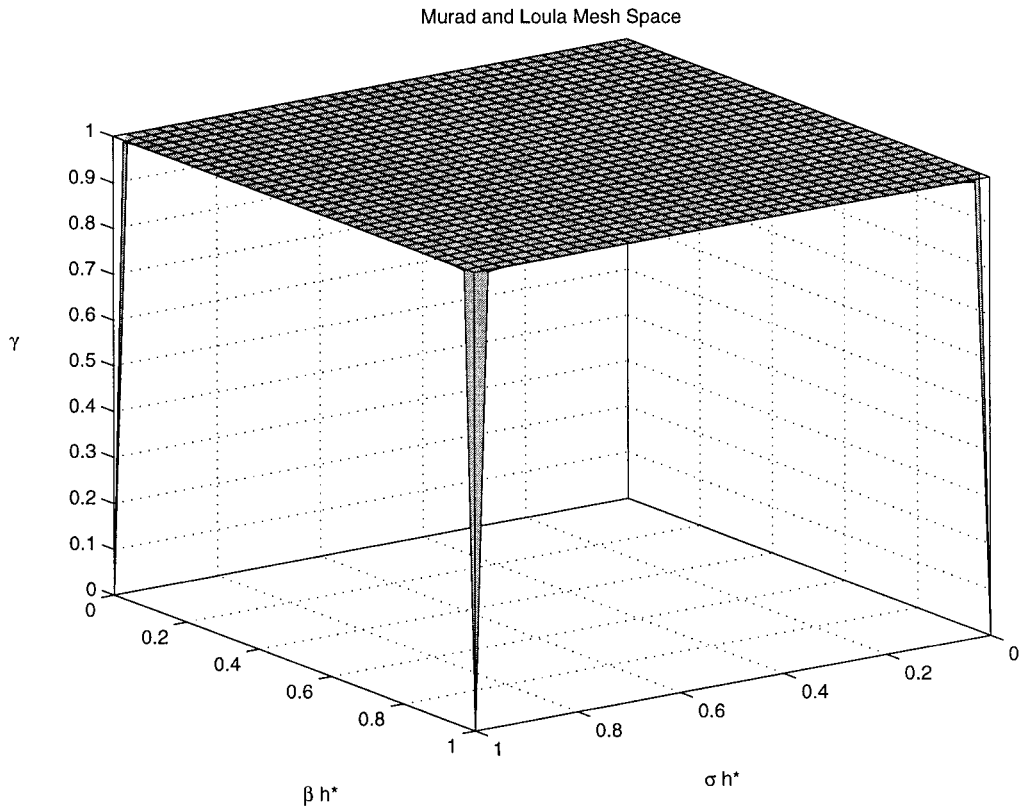

Figure 10. Stability plane for comparing Murad and Loula results ($T_f = 6{\cdot}1e-7$, $T_g = \infty$, $v = 0{\cdot}2$, $\theta = 1$)

Factor, T_g, and the weighting between explicit and implicit information, θ . It is shown that Biot's equations for saturated and unsaturated media must be solved with an implicitly dominated scheme (i.e. $\theta > 0{\cdot}5$) unless the system is completely decoupled. The results also indicate that in order to avoid all temporal oscillations in a saturated medium, the time stepping scheme must be fully implicit (i.e. $\theta = 1{\cdot}0$). Further, the presence and persistence of spatial oscillations in the pore pressure solution are governed by the ratio of the time-step to the square of the space-step for a fixed set of physical property values and time-integration weighting. Hence, the notorious problem of early-time spatial oscillations in the pore pressure must be considered in terms of both the time step and the mesh discretization. In addition, special cases arise which do allow accurate, semi-implicit time stepping by decreasing either the Time Factor or Void Factor. However, a breakdown in Von Neumann analysis is shown to occur for unsaturated media (i.e. $T_g \ll T_f$) as a result of unaccounted boundary conditions which limits the ability to manipulate the Void Factor to produce gains in computational performance. The analysis also predicts oscillations resulting from the incorrect initial incompressibility constraint, as reported by Murad and Loula for certain spatial/temporal discretizations. Finally, performing this analysis provides an improved understanding of FEM solutions generated for Biot's general theory of consolidation and makes available guidelines for parameter selections in practical consolidation computations on finite elements.

ACKNOWLEDGEMENT

This work was supported by National Institutes of Health grant R01-NS33900 awarded by the National Institute of Neurological Disorders and Stroke.

REFERENCES

1. T. W. Lambe, *Soil Mechanics*, *SI Version*, Wiley, New York, 1979.
2. K. Terzaghi, *Theoretical Soil Mechanics*, Wiley, New York, 1942.
3. M. Biot, 'General theory of three dimensional consolidation', *J. Appl. Phys.*, **12,** 155–164 (1941).
4. Y. Tada and T. Nagashima, 'Modeling and simulation of brain lesions by the finite-element method', *IEEE Eng. Med. Bio.*, 497–503 (1994).
5. T. Nagashima, T. Shirakuni and SI. Rapoport, 'A two-dimensional, finite element analysis of vasogenic brain edema,' *Neurol. Med. Chir.*, **30,** 1–9 (1990).
6. T. Nagashima, Y. Tada, S. Hamano, M. Skakakura, K. Masaoka, N. Tamaki and S. Matsumoto, 'The finite element analysis of brain oedema associated with intracranial meningiomas', *Acta. Neurochir.* (Suppl.), **51,** 155–7 (1990).
7. P. J. Basser, 'Interstitial pressure, volume, and flow during infusion into brain tissue', *Microvasc. Res.*, **44,** 143–65 (1992).
8. C. T. Hwang, N. R. Morgenstern and D. W. Murray, 'On solutions of plane strain consolidation problems by finite element methods', *Can. Geotech. J.*, **8,** 109–118 (1971).
9. C. T. Hwang, N. R. Morgenstern and D. W. Murray, 'Application of the finite element method to consolidation problems', *Symp. on Applications of the Finite Element Method in Geotechnical Engineering*, U. S. Army Engineering Waterways Experiment Station, Vicksburg, MI, pp. 1972, 739–765.
10. J. Booker and J. C. Small, 'An investigation of the stability of numerical solutions of Biot's equations of consolidation', *Int. J. Solid Struct.*, **11,** 907–917 (1975).
11. M. Murad and A. Loula, 'Improved accuracy in finite element analysis of Biot's consolidation problem', *Comput. Meth. Appl. Mech. Engng.*, **95,** 359–382 (1992).
12. M. Murad and A. Loula, 'On stability and convergence of finite element approximations of Biot's consolidation problem', *Int. J. Numer. Meth. Engng.*, **37,** 645–667 (1994).
13. C. Taylor and P. Hood, 'A numerical solution of the Navier–Stokes equations using the finite element technique', *Comput. Fluids*, **1,** 73–100 (1973).
14. P. Hood and C. Taylor, 'Navier–Stokes equations using mixed interpolation', in *Finite Element Methods in Flow Problems*, J. T. Oden, O. C. Zienkiewicz, R. H. Gallagher and C. Taylor (eds.), 1974, pp. 121–132.
15. M. I. Miga, K. D. Paulsen, F. E. Kennedy, P. J. Hoopes, A. Hartov and D. W. Roberts, 'A 3D brain deformation model experiencing comparable surgical loads', *Proc. 19th An. Int. Conf. IEEE Engng. Med. Biology Soc.*, 1997, pp. 773–776.
16. K. D. Paulsen, M. I. Miga, F. E. Kennedy, P. J. Hoopes, A. Hartov and D. W. Roberts, 'A computational model for tracking subsurface tissue deformation during stereotactic neurosurgery', *IEEE Trans. Biomedical Engng.*, 1998, in press.
17. L. Lapidus and G. F. Pinder, *Numerical Solution of Partial Differential Equations in Science and Engineering*, Wiley, New York, 1982.
18. D. R. Lynch and K. D. Paulsen, 'Origin of vector parasites in numerical maxwell solutions', *IEEE Trans. Microwave Theory Techn.*, **39,** 383–394 (1991).

